Pergamon

Tetrahedron 56 (2000) 6913–6925

TETRAHEDRON

Mediation of Photochemical Reactions of 1-Naphthyl Phenylacylates by Polyolefin Films. A 'Radical Clock' to Measure Rates of Radical-Pair Cage Recombinations in 'Viscous Space'

Weiqiang Gu and Richard G. Weiss*

Department of Chemistry, Georgetown University, Washington, DC 20057-1227, USA

Received 1 February 2000; revised 20 March 2000; accepted 22 March 2000

Abstract—The fates of phenylacyl/1-naphthoxy singlet radical pairs generated upon irradiation of 1-naphthyl phenylacetate (**1a**) and 1-naphthyl 2-phenylpropanoate (**1b**) in three unstretched and stretched polyethylene films and isotactic and syndiotactic polypropylene films have been investigated. From dynamic fluorescence measurements, the primary locus of reactions by **1** is within amorphous regions of the films. The reaction cages afforded by these media inhibit escape of the radical pairs and mediate their reorientational motions leading to photo-Fries and related products. In essence, the cages act as stiff-walled templates. In addition, a method is described to measure the rate constants for the singlet radical pairs. Thus, the rate constants (leading to the keto precursors) of the 2-phenylacyl-1-naphthols from the radical pairs of **1** ($>10^8\ s^{-1}$) are >6 times the rate constants for the 4-isomers. Film stretching increases this selectivity but there is no obvious correlation between the rate of the in-cage radical pair recombinations and macroscopic polymer, properties such as degree of crystallinity and frequency of branched chains. By contrast, formation of (the keto precursors of) 2-benzylic-1-naphthols (from in-cage recombinations after phenylacyl decarbonylation) is slower than for the 4-benzyl-1-naphthols.

Introduction

For several years, we have investigated the static and dynamic properties of reaction cages afforded to a variety of guest molecules by anisotropic media,[1] including polyolefin films.[2] The notion of a cage has been refined over the last 65 years, since the pioneering work of Rabinowitch and coworkers.[3] However, even now, its definition differs depending upon the nature of the system.[4] Our prior investigations have provided information concerning the size, shape, and wall flexibility of polyolefin cages as well as micro- and macro-scopic diffusion rates and rates of conformational changes of guest molecules within them.[1] The dynamics and trajectories of motions of two species sequestered initially within one polyolefin cage have not been investigated. We describe here a method for doing so in three films of unstretched and stretched polyethylene (**PE**) that differ in degree of crystallinity and in isotactic and syndiotactic polypropylene (**PPP**). Our monitors are the relative product yields generated from irradiation of two naphthyl esters, 1-naphthyl phenylacetate (**1a**) and 1-naphthyl 2-phenylpropanoate (**1b**) (Eq. (1)[2a,5]), and radical-pair

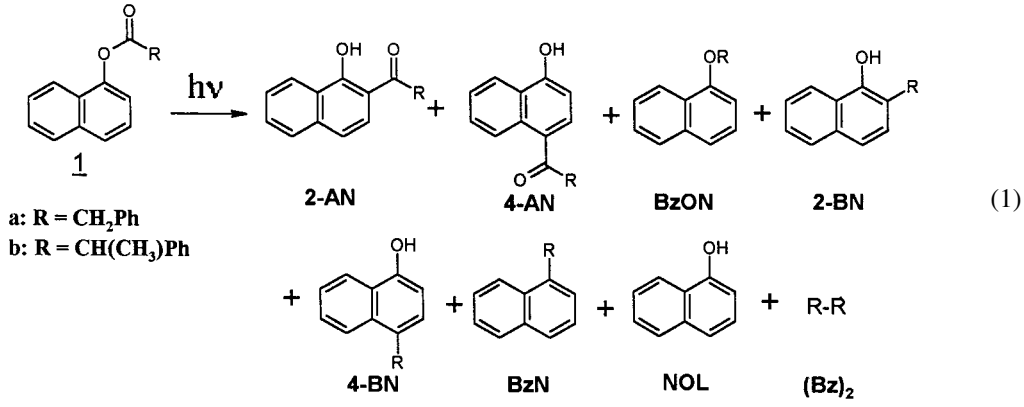

(1)

Keywords: 1-naphthyl phenylacetate; photo-Fries rearrangements; polyolefin films; radical clock.

* Corresponding author. Tel.: +1-202-687-6013; fax: +1-202-687-6209; e-mail: weissr@gusun.georgetown.edu

0040–4020/00/$ - see front matter
PII: S0040-4020(00)00512-3

recombination rates that are based upon the decarbonylation of phenylacyl radicals as a 'clock'.

'Radical clocks' provide a simple, inexpensive alternative to direct spectroscopic methods for measuring rates of reaction of short-lived intermediates.[6] The utility of any clock is limited by its intrinsic time frame;[7] the response must be concurrent with the process being investigated. Although some radical clocks operate on time scales shorter than one picosecond,[8] it would be useful to extend the time domain in which a particular clock operates since many, such as the ones employed here, are limited to specific applications.[9] In 'normal' (i.e. low-viscosity and isotropic) media, less than one nanosecond is required for the recombination of singlet radical pairs generated in a cage,[10] including when the radicals are generated during the photo-Fries type rearrangements of esters like **1**.[11,12] Decarbonylation of a phenylacyl radical from **1a** or **1b** is too slow to compete with these recombination rates.[10,13] However, the (anisotropic) viscous space provided by polyolefin cages should slow and direct the world *around* an acyl clock without affecting the rate of its decarbonylation; kinetic information on the recombination of phenylacyl/1-naphthoxy radical pairs from **1** should become available.

Results

General sample preparations, irradiations, and analytical procedures

Polyethylene and polypropylene films were immersed for protracted periods in chloroform and cyclohexane, respectively, to remove antioxidants and plasticizers included by the manufacturers. The cleaned films imbibed 3–7 mmol/kg dopant when placed in 10–20 mM 1-naphthyl ester solutions. After the doped films were irradiated at >300 nm under nitrogen, photoproducts were removed efficiently by extraction in several aliquots of the doping solvent. Mass balances were >85% as indicated by quantitative GC analyses. Relative product yields (normalized to 100%) and percent conversions of **1** by GC analyses assume that all species have the same detector response. During HPLC analyses, peak areas were divided by the appropriate molar extinction coefficients at 254 nm to convert them to relative product yields and conversions.

Irradiations in polymer films

Esters **1a** and **1b** were irradiated in unstretched and stretched **PE** (**NDLDPE**, **BHDPE**, and **LLDPE**; see Experimental part for characterization of each) and unstretched isotactic **PPP** (*iso*-**PPP**) and syndiotactic **PPP** (*syn*-**PPP**). The relative photoproduct yields (Table 1) are the averages from at least nine separate analyses (≥3 runs and ≥3 chromatograms/run; precision errors are one standard deviation). The relative product yields were invariant (within the limits of experimental error) to ca. 30% conversion of **1**. In all cases, no 1,2-diphenylethane from **1a** or 2,3-diphenylbutane from **1b** (**(Bz)$_2$**) was found under the irradiation conditions reported. **2-AN**, the major product, is always at least six times the yield of **4-AN.** The low relative yields (≤4% in all of the experiments in films) and broad peaks of 1-naphthol (**NOL**) in our chromatographic analyses made it more difficult to quantify than the other photoproducts in Eq. (1).

The influence of temperature on photoreactions of **1b** has been studied also in unstretched and stretched **NDLDPE** and unstretched **BHDPE** films over a range (5–60°C) that does not include any phase transitions.[14] It is above the glass transition temperature and below the crystal melting temperature. The irradiation temperature of the **PPP** samples, 5°C, is above the glass transition temperature.[15] Both the [**2-AN**]/[**4-AN**] ratios and total relative yields of decarbonylation products are consistently larger at lower temperatures. Since phenylacyl decarbonylation rates decrease with decreasing temperature, the unexpected *increase* of **BN** and **BzON** products must be related to interactions of the radicals with their polymeric environments.

Table 1. Relative yields (%) of selected photoproducts from 3–7 mmol/kg **1a** and **1b** in unstretched (u) and stretched (s) polyolefinic films. The relative yield of **NOL** was always <4%

1	Film	*T* (°C)	2-AN	4-AN	2-BN	4-BN	BzON
a	**NDLDPE**(u)	22	85.8±1.5	7.4±1.4	1.2±0.3	1.6±0.3	<0.2
	NDLDPE(s)	22	82.9±2.2	6.9±1.2	1.1±0.3	1.4±0.3	<0.2
	BHDPE(u)	22	87.9±0.4	5.8±0.9	0.9±0.3	1.3±0.1	<0.2
	BHDPE(s)	22	82.0±1.1	5.4±0.8	1.9±0.3	2.1±0.3	<0.2
b	**NDLDPE**(u)	5	84.4±1.4	5.6±0.7	1.1±0.2	3.0±0.2	1.5±0.5
		22	82.7±0.8	6.3±1.1	1.2±0.7	3.5±0.9	1.7±0.3
		40	78.9±1.1	10.1±1.0	1.5±0.3	2.8±0.1	2.0±0.2
		60	74.9±1.0	13.0±1.5	1.8±0.6	3.5±0.2	1.9±0.3
	NDLDPE(s)	5	56.9±1.5	4.0±0.2	8.8±0.3	11.7±1.6	7.3±0.6
		22	74.7±1.4	6.0±1.5	2.7±0.2	8.0±0.5	3.0±0.5
		40	70.7±1.9	8.5±0.4	3.8±0.3	7.4±0.8	3.1±0.3
		60	72.2±0.4	11.6±0.8	1.4±0.2	5.6±0.3	2.3±0.1
	BHDPE(u)	5	73.5±2.7	6.6±1.2	1.7±0.3	6.6±0.4	3.7±0.8
		22	79.1±1.0	6.9±0.5	1.1±0.7	5.0±0.6	2.9±0.7
		40	80.0±0.9	8.1±0.9	0.9±0.2	2.8±0.1	2.1±0.4
		60	77.5±1.0	12.7±1.2	1.5±0.2	3.1±0.2	2.2±0.2
	BHDPE(s)	22	66.2±1.0	5.5±0.1	4.3±1.3	10.9±1.8	4.6±0.3
	LLDPE(u)	5	80.0±0.2	9.3±0.5	0.6±0.2	3.0±0.2	2.1±0.1
	LLDPE(s)	5	65.1±0.8	8.5±0.5	3.7±0.2	8.3±0.8	4.4±0.2
	iso-**PPP**(u)	5	78.0±1.0	12.5±0.5	1.9±0.3	3.6±0.4	1.7±0.4
	syn-**PPP**(u)	5	75.2±0.2	9.3±0.1	2.7±0.6	6.0±0.2	2.5±0.5

Table 2. Relative yields of photoproducts from irradiations of 2 mM **1a** or **1b** in isotropic media

1	Medium	T (°C)	2-AN	4-AN	2-BN	4-BN	BzON	BzN	NOL	$(Bz)_2$
a	Hexane	22	44.1±0.6	17.5±0.5	9.9±0.1	10.6±0.1	1.5±0.1	1.0±0.1	10.8±0.3	4.6±0.1
		5	45.4±2.5	17.9±0.7	6.6±0.3	8.0±0.6	1.0±0.1	1.2±0.1	15.4±0.9	4.6±0.3
	t-Butyl alcohol	26	89.2±0.8	3.8±0.5	0.7±0.1	0.6±0.1	0	0	2.8±0.8	2.9±0.5
b	Hexane	22	44.6±0.7	16.6±1.6	8.0±0.2	17.0±0.6	3.0±0.3	0.6±0.1	5.1±0.5	5.1±0.2
		5	52.5±1.5	18.7±2.7	5.2±0.7	11.3±0.7	3.0±0.2	0.4±0.1	5.7±0.2	3.2±0.1
	t-Butyl alcohol	26	87.2±1.0	3.3±0.5	0.8±0.2	1.1±0.2	0.8±0.2	0	4.0±0.2	2.8±0.7

Influence of polyolefin structure, crystallinity, and stretching on the photochemistry of 1

The polymeric chains of **NDLDPE** have more short branches than those of **BHDPE**.[14] Unfortunately, the three polyethylenes also differ in degree of crystallinity, but in a different order: **BHDPE**>**NDLDPE**>**LLDPE**. The *iso*-**PPP** and *syn*-**PPP** films have methyl groups arranged regularly along polymethylene chains; there are many more, but shorter, (methyl) branches than in the **PE** films. In the unstretched films, [**2-AN**]/[**4-AN**] ratios from **1b** are lowest in **LLDPE** and the two **PPP**s and distinctly higher in the other two **PE** types; where comparisons are possible, ratios from **1a** and **1b** are similar. For physical interpretations, it may be better to group the reactions of benzylic radicals at the 1-naphthoxy positions near initial ester lysis (i.e. at oxygen and C-2) and remote from it (i.e. at C-4): ([**2-BN**]+[**BzON**])/[**4-BN**] ratios are nearly constant (ca. 0.7–1.0) in all of the unstretched films at 22°C, but they are at least six times smaller than [**2-AN**]/[**4-AN**]. There is no obvious correlation between photoproduct ratios and either polymer branching or crystallinity.

Film stretching is known to increase somewhat the degree of crystallinity[16] and decrease the free volumes of cages.[17] It has very little influence on the [**2-AN**]/[**4-AN**] or ([**2-BN**]+[**BzON**])/[**4-BN**] ratios. However, except for **1a** in **NDLDPE**, film stretching increases markedly the relative yields of [**2-BN**]+[**BzON**]+[**4-BN**], the total yield of the three in-cage decarbonylation products (vide infra).

Irradiations in isotropic solutions

Both **1a** and **1b** were also irradiated in hexane and *t*-butyl alcohol (Table 2). The distributions of photoproducts from **1a** and **1b** are similar in the same solvent. When the solvent is changed from hexane to *t*-butyl alcohol, the ratios of [**2-AN**]/[**4-AN**] increase and the relative yields of decarbonylation products decrease. At the same time, there is a decrease of cage-escape products, **NOL** and $(Bz)_2$. In hexane, decreasing temperature from 22 to 5°C has no discernible effect on the [**2-AN**]/[**4-AN**] ratios from **1a** (2.5) and **1b** (2.7–2.8), but the total relative yield of decarbonylation products, [**2-BN**]+[**4-BN**]+[**BzON**], is *decreased significantly* (from 22 to 15.6% for **1a** and from 28 to 19.5% for **1b**). These results are in marked contrast to the trends observed upon reducing temperature in polyolefin films (vide ante). Some irradiations were also performed in a more viscous *n*-alkane, dodecane. The relative yields of the photoproducts that could be analyzed are more similar to those in *t*-butyl alcohol than in hexane; **NOL** and $(Bz)_2$ could not be separated from the solvent peak during GC analyses. At room temperature in dodecane, [**2-AN**]/[**4-AN**] is 9 (**1a**) or 8 (**1b**) and [**2-BN**]/[**4-BN**]/[**BzON**] was 1/1.3/0.3 (**1a**) or 1/1.6/1.1 (**1b**).

Irradiations of 1a in the presence of thiophenol

Thiophenol, a good hydrogen atom donor,[18] can intercept efficiently radicals from **1** that escape from their initial cages. The consequences of this trapping are shown in Fig. 1. When thiophenol concentrations were high, ([**2-BN**]+[**4-BN**]+[**BzON**])/([**2-AN**]+[**4-AN**]) ratios

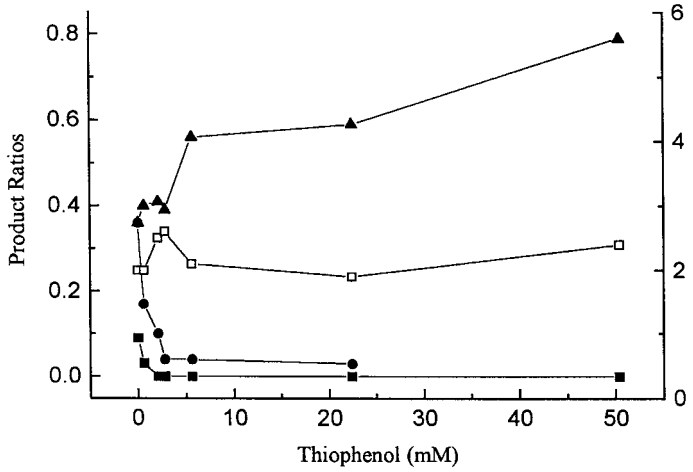

Figure 1. Selected photoproduct ratios from irradiations of hexane solutions of **1a** in the presence of thiophenol: (●, left axis) ([**2-BN**]+[**4-BN**] +[**BzON**])/([**2-AN**]+[**4-AN**]); (▲, left axis) [**NOL**]/([**2-AN**]+[**4-AN**]); (■, left axis) [$(Bz)_2$]/([**2-AN**]+[**4-AN**]); (□, right axis) [**2-AN**]/[**4-AN**]. The small rise and fall of the [**2-AN**]/[**4-AN**] ratios at low thiophenol concentrations is reproducible; its cause has not been pursued.

could not be determined due to small peaks that partially overlapped those for decarbonylation products in GC profiles. Both [**(Bz)$_2$**]/([**2-AN**]+[**4-AN**]) and ([**2-BN**]+[**4-BN**]+[**BzON**])/([**2-AN**]+[**4-AN**]) decrease with increasing thiophenol concentration while [**NOL**]/([**2-AN**]+[**4-AN**]) increases. At the same time, the ratios of [**2-AN**]/[**4-AN**] remain relatively constant.

Attempted sensitization of 1a photoreactions by benzophenone triplets

To determine whether **1** can react in part from the lowest energy triplet state, benzophenone was irradiated in the presence of **1a** (see Experimental section). Under conditions for which >80% of the benzophenone in the benzophenone/benzhydrol solution was lost and significant amounts of benzopinacol were formed,[19] *no* benzopinacol or photo-Fries products or loss of benzophenone was detected from the benzophenone/benzhydrol solution containing **1a**. These results demonstrate that **1a** is an efficient quencher of benzophenone triplet states. In addition, the triplet state energies of benzophenone (289.5 kJ/mol[20]), 1-naphthyl acetate (251.8 kJ/mol[21]), and 1-naphthyl 2-methyl-2-phenylpropanoate (249 kJ/mol, as estimated from its lowest wavelength phosphorescence peak[12]) indicate that **1a** should be excited efficiently by benzophenone triplets. The lowest triplet state of **1a** is unreactive. The participation of an upper triplet state in the reactions is unlikely, but it cannot be excluded on the basis of these experiments.

Determination of fluorescence decay constants for 1 in hexane and in two polyolefin films

All decay curves were accumulated as time-correlated single photon counting histograms using one excitation wavelength (280 nm) and three emission wavelengths (325, 334, and 339 nm). The curves for one sample were analyzed individually and then globally. The global results are described here. In degassed hexane solutions, the dynamic fluorescence can be fit reasonably well to single exponential decays: $\tau \cong 11.6$ ns for **1a** and $\cong 10.3$ ns for **1b**. *Two* constants are necessary to fit the decays from **1a** and **1b** in **NDLDPE** and **BHDPE**, the only polyolefin media examined in this way.

The shorter decay components of **1a**, $\tau_s \approx 8$ ns, represent ca. 90% of the total fluorescence in unstretched **NDLDPE** and ca. 75% in the stretched film. Consistently, stretching increased slightly (ca. 0.5 ns) τ_s and the longer component, $\tau_l \approx 18$ ns. In **BHDPE**, the decay constants were slightly smaller than in **NDLDPE**, but larger increases to τ_s and τ_l (0.7 and 3.9 ns, respectively) were observed upon film stretching and the relative importance of the shorter component decreased from ca. 80% to ca. 70% of the total.

Although the decay constants for **1b** and their changes upon film stretching were very similar to those for **1a**, the relative importances of the shorter component were somewhat smaller: in **NDLDPE**, ca. 80% (u)→70% (s); in **BHDPE**, ca. 65% (u)→60% (s).

Discussion

The photo-Fries reaction[21,22,23]

The kinetic steps pertinent in our work to the reactions of **1** in the polyolefin films are shown in Scheme 1. It includes mechanisms for formation of all products detected and is consistent with the results from the thiophenol trapping experiments. It excludes some photophysical processes, such as fluorescence from ^{1}**1** states and ^{1}**1**→^{3}**1**→**1** intersystem crossing. Our 'clock' (**k$_{-CO}$**) is started by homolysis of the (O═)C–O bond from ^{1}**1** states[21,23] to generate a phenylacyl and a 1-naphthoxy radical pair. The inability of reactions of **1a** and 1-naphthyl acetate to be sensitized by benzophenone triplet states in hexane solutions under conditions where photoreduction of benzophenone by added benzhydrol is completely suppressed[19] agrees with the prior attribution of the photo-Fries reaction to the singlet manifold.[23,24]

In-cage radical pair rearrangement to form 2- and 4-phenylacyl-1-naphthols, **2-AN** and **4-AN**, after enolization of the original keto intermediates,[23] competes with reformation of **1** and cage escape. The latter leads to a mixture of radical

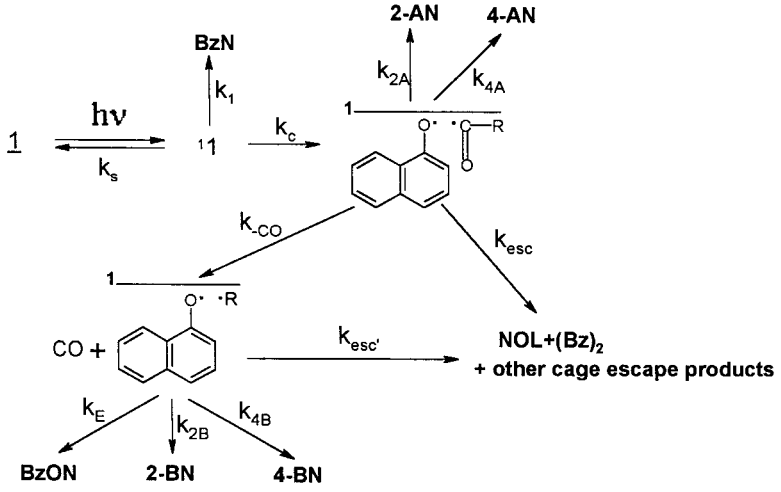

Scheme 1.

trapping products (e.g. **NOL**) when 1-naphthoxy radicals abstract hydrogen atoms from a host matrix[14]) and coupled radicals (e.g. **2**- and **4-BN**, **BzON**, and the benzylic dimer, **$(Bz)_2$**). In addition, some of the **BN**, and **BzON** may be formed in-cage if the rate of cage escape is slower than the rate of phenylacyl decarbonylation when it occurs (vide infra). The decarboxylation process leading to **BzN**[25] affects the absolute yields of **AN**, **BN**, **BzON**, **NOL**, and the other products in Eq. (1), but not their yields relative to each other or their rate constants for formation.

Formation of the 'normal' photo-Fries products, the **AN** isomers, is environmentally mediated (i.e. sensitive to the size, shape, and wall flexibility of the reaction cages[1]). The disparity between the selectivities of **AN** and **BN** isomer formations is not explained by different intrinsic rates of reaction of benzylic and phenylacyl radicals: in the only clear comparison of addition rates of a carbonylated/decarbonylated radical set to a common substrate we have found, the decarbonylated radical, *t*-butyl, reacts *more* rapidly with acrylonitrile than its carbonylated analogue, pivaloyl.[26]

Alternatively, the relative positions (with respect to a 1-naphthoxy radical) at which the phenylacyl and benzylic radicals are created may mandate which product isomer is formed eventually. The period between lysis of ^{1}**1** and decarbonylation may permit most of the orientational effects of the initial radical pair to be lost before 1-naphthoxy and benzylic radicals combine.[27] To test this possibility, [**2-BN**]/[**4-BN**] ratios from benzyl 1-naphthyl ether (**BzONa**) were measured.[28] Lysis of **BzONa** allows a 'decarbonylated' radical pair to begin its existence with the two radical centers oriented like a carbonylated radical pair (from **1**). In the films, as well as in cyclohexane, [**2-BN**]/[**4-BN**] from **BzONa** is near **2**. These results indicate that the ([**2-BN**]+[**BzON**])/[**4-BN**]) ratios from **1** in films are from combinations of radical pairs that are closer to being spatially equilibrated than their phenylacyl/1-naphthoxy analogues. Initial relative positions and orientations of the radical pairs in films contribute to (but are *not* the sole source of) the disparities between the [**2-AN**]/[**4-AN**] and [**2-BN**]/[**4-BN**] (or ([**2-BN**]+[**BzON**])/[**4-BN**]) ratios.

The decarbonylation step

The stopping point of our clock is marked by decarbonylation of a phenylacyl radical. Although $\mathbf{k_{-CO}}$ is dependent upon temperature and to a lesser extent on solvent polarity,[29] it does not appear to be sensitive to medium viscosity. This conclusion is based on decarbonylation rates of pivaloyl which are nearly the same in hexane and tetradecane[29] and *decarboxylation* rates which have been shown to be invariant in paraffins from hexane to octadecane.[30] Thus, we assume that $\mathbf{k_{-CO}}$ in isooctane and the polyolefinic films are the same. At 22°C in isooctane, $\mathbf{k_{-CO}}$ is 4.8×10^6 s^{-1} for phenylacetyl (from **1a**) and 4.0×10^7 s^{-1} for 2-phenylpropanoyl (from **1b**).[13] The nearly one order of magnitude of difference in rates for these two phenylacyl radicals results in more decarbonylation products from **1b** than **1a** in the polyolefinic films (Table 1).

The reverse step, addition of CO to a benzylic radical (to reform phenylacyl), cannot compete with radical-pair combinations. The activation energy for carbonylation of a primary radical is 6.0 kcal/mol in benzene solution,[9d] and the rate of addition of CO to benzyl is much slower than to a primary radical. Carbon monoxide is a passive observer even if it remains inside the polyolefin cages for the duration of the radical-pair reactions.

However, its presence may inhibit some motions of the radical pair because it can occupy crucial space within a cage needed to attain product-forming transition states. The vectoral distance (d) traveled by a CO molecule from the locus of its formation in the radical-pair cage during a period of time (t) can be approximated from knowledge of the diffusion coefficients (D)[31a] and the simple expression, $d=(2Dt)^{1/2}$.[31b] On this basis, a molecule of CO is able to move <5 Å during 1 ns and >10 Å during 100 ns in the polyolefinic films. These distances/times are intermediate between CO remaining within and effectively escaping from a cage containing a benzylic/1-naphthoxy radical pair.

Experimental differentiation of in-cage and out-of-cage reactions

Given the low dopant concentrations and low light fluxes employed, no more than one radical pair should occupy one cage at any time. As a result, **$(Bz)_2$** is the only radical recombination photoproduct in Scheme 1 that must be from out-of-cage reactions; the two radicals from which it forms arise from two different molecules of **1**.

The presence of significant amounts of **$(Bz)_2$** indicates that the **BN** and **BzON** from irradiations of either **1a** or **1b** in N_2-saturated hexane derive mainly from out-of-cage recombinations of the initially formed radical pairs. In hexane, the other recombination photoproducts, **2-AN** and **4-AN**, must be formed almost exclusively by in-cage processes based on results from the experiments in the presence of benzenethiol.[18] No **$(Bz)_2$** was detected from irradiation of **1a** in the presence of 2×10^{-2} M benzenethiol because benzylic radicals that escape from their initial hexane cages are scavenged by thiol more rapidly than they can find another radical fragment from **1**. The [**2-AN**]/[**4-AN**] ratio was constant and the [**BN**]/[**AN**] ratio approached zero as the thiol concentration was increased further, the **AN** products must be formed in-cage even in hexane. *The presence of **$(Bz)_2$** (in the absence of benzenethiol) is our indicator that some of the **BN** and **BzON** is derived from combination of radicals which have escaped from their initial cages. Its absence is evidence that no out-of-cage radical pair recombinations are occurring.*

Irradiations of **1** in the polyolefin films yield some **BN** and **BzON**, *but no discernible **$(Bz)_2$** coupling product*. The absence of **$(Bz)_2$** is strong evidence that **BN** and **BzON** are formed in-cage. In the polymeric media, radicals which escape from their initial cages must be scavenged efficiently by trap sites, such as unsaturated groups and easily abstractable hydrogen atoms,[14] which serve the function of benzenethiol in hexane solutions. The scavenged product from 1-naphthoxy radicals is **NOL**; due to experimental difficulties, no attempts to quantify the scavenged

Table 3. Calculated rate constants and rate constant ratios for formation of selected photoproducts from 3–7 mmol/kg **1a** and **1b** in unstretched (u) and stretched (s) polyolefinic films

1	Film	T (°C)	$10^{-8}\mathbf{k_{2A}}$ (s^{-1})	$10^{-7}\mathbf{k_{4A}}$ (s^{-1})	$\mathbf{k_{2A}/k_{4A}}$	$\mathbf{k_{2B}/k_{4B}/k_E}$
a	**NDLDPE**(u)	22	1.5	1.3	12	1/1.3/<0.2
	NDLDPE(s)	22	1.6	1.4	12	1/1.3/<0.2
	BHDPE(u)	22	2.0	1.3	15	1/1.4/<0.2
	BHDPE(s)	22	1.0	0.7	15	1/1.1/<0.2
b	**NDLDPE**(u)	5	3.2	2.1	15	1/2.7/1.4
		22	5.1	3.9	13	1/2.9/1.4
		40	9.3	12	8	1/1.9/1.3
		60	14	25	6	1/1.9/1.1
	NDLDPE(s)	5	0.43	0.32	14	1/1.3/0.8
		22	2.2	1.7	13	1/3.0/1.1
		40	3.7	4.4	8	1/1.9/0.8
		60	10	17	6	1/4/1.6
	BHDPE(u)	5	1.3	1.2	11	1/3.9/2.2
		22	3.5	3.1	12	1/4.5/2.6
		40	10	10	10	1/3.1/2.3
		60	16	25	6	1/2.1/1.5
	BHDPE(s)	22	1.3	1.1	12	1/2.5/1.1
	LLDPE(u)	5	3.0	3.5	9	1/5.0/3.5
	LLDPE(s)	5	0.84	1.1	8	1/2.2/1.2
	iso-**PPP**(u)	5	2.3	3.7	6	1/1.9/0.9
	syn-**PPP**(u)	5	1.4	1.8	8	1/2.2/0.9

products from phenylacyl or benzylic radicals, the other part of the initial pair, were made.

A model for kinetic analyses in the polyolefinic films

If all of the **AN**, **BN**, and **BzON** photoproducts emanate from in-cage processes and there are no secondary photoreactions, expressions for $\mathbf{k_{2A}}$ and $\mathbf{k_{4A}}$ (Eqs. (2) and (3)) can be derived using the mechanism in Scheme 1. The constancy of the relative yields in the films up to 30% conversion of **1** is evidence that secondary photoreactions are negligible, and the absence of detectable $\mathbf{(Bz)_2}$ indicates that the photoproducts in Eqs. (2) and (3) are from in-cage reactions. Thus, the necessary conditions are met. Besides the relative yields of the photoproducts, only the absolute values of $\mathbf{k_{-CO}}$ are necessary to calculate $\mathbf{k_{2A}}$ and $\mathbf{k_{4A}}$. For reasons discussed above,[29,30] the $\mathbf{k_{-CO}}$ are from decarbonylations of the appropriate phenylacyl radicals in isooctane.[13] Due to the uncertainty of the origin of **NOL** (i.e. the extent to which the $\mathbf{k_{esc'}}$ path participates), Eqs. (2) and (3) are only approximately correct; the absolute values of $\mathbf{k_{2A}}$ and $\mathbf{k_{4A}}$ may be overestimated by ≤5%. However, the $\mathbf{k_{2A}/k_{4A}}$ (=[**2-AN**]/[**4-AN**]) and $\mathbf{k_{2B}/k_{4B}/k_E}$ (=[**2-BN**]/[**4-BN**]/[**BzON**]) ratios do not depend on the origin of **NOL**.

$$\mathbf{k_{2A}} \cong \mathbf{k_{-CO}}[\textbf{2-AN}]/\{[\textbf{2-BN}] + [\textbf{4-BN}] + [\textbf{BzON}]\} \quad (2)$$

$$\mathbf{k_{4A}} \cong \mathbf{k_{-CO}}[\text{4-}\textbf{AN}]/\{[\textbf{2-BN}] + [\textbf{4-BN}] + [\textbf{BzON}]\} \quad (3)$$

The general nature and number of reaction cage types in the polyolefin media

A simple explanation for the constancy of the relative photoproduct yields with conversion is that the occupied cages within one polyolefin film are very similar. The data are equally consistent with the presence of more than one site type *if* the molecules of **1** have the same molar extinction coefficients and quantum yields for reaction in all of the site types, or molecules in all but one site type do not undergo photo-Fries type reactions. Analyses of only the photoproduct mixtures do not allow these possibilities to be distinguished. However, multi-site models are frequently invoked to explain reactivity patterns and spectroscopic properties of guest molecules in heterogeneous media,[1] including polyolefin films.[5,32]

The fluorescence decay measurements suggest that molecules of **1** do reside in more than one (distinguishable) cage type in the polyolefin films. It is unwise to convert the relative percentages of τ_l and τ_s in the decay histograms into mole fractions of cage occupancies because the quantum efficiency of fluorescence from ^{1}**1** in each cage type is unknown. However, the decay percentages and their changes upon film stretching do provide a *qualitative* measure of the occupancies. The fluorescence data are consistent with a model in which some molecules of **1** reside in the amorphous part and others are along crystalline–amorphous interfaces of the films.[32] Since film stretching tends to translocate dopant molecules like **1** from amorphous to interfacial sites,[32] we associate the molecules with τ_l to the (more rigid) interfacial sites and those with τ_s to the (less rigid) amorphous ones. Due to the proximity of crystalline chains in interfacial regions, the walls of their cages are stiffer than those of the amorphous cages and, therefore, should inhibit conformational motions of ^{1}**1** states to a greater extent.

On this basis, the majority of molecules of **1** resides (and reacts) in cages within the amorphous part, even in stretched films. Thus, one of the limiting conditions described above for a multi-site model must be operative. For the purposes of discussion, we will assume that only one of the cage types, probably that in the amorphous regions of the films, allows photoreactions of **1**. In fact, the much longer lifetimes of ^{1}**1** states in interfacial cages may be a consequence of much less efficient lysis ($\mathbf{k_l}$ and $\mathbf{k_c}$ in Scheme 1); we have been unable as yet to test this possibility. Regardless, the several nanosecond lifetimes for molecules in amorphous cages

Table 4. Activation parameters for formation of **2-AN** and **4-AN** from **1b** in **PE** films

Film	$Ea_{2\text{-AN}}$ (kJ/mol)	log(*A*) log(s^{-1})	$Ea_{4\text{-AN}}$ (kJ/mol)	log(*A*) log(s^{-1})
NDLDPE(u)	21.3±0.8	12.6±0.2	34.7±2.9	13.9±0.5
NDLDPE(s)	42.6±5.9	15.7±1.0	53.5±2.9	16.6±0.5
BHDPE(u)	41.2±3.3	14.9±0.6	43.1±2.9	15.2±0.5

indicates that they are able to explore several conformations in their excited singlet states before reacting (N.B., following the pathways initiated by $\mathbf{k}_c$). The nature of those motions and those of the biradical pairs produced upon lysis of ^{1}**1** will be mediated by steric constraints imposed by the size, shape, and wall stiffness of the cages.[1]

The relative preference of a phenyacyl radicals to add to the 2- or 4-position of a 1-naphthoxy radical can be assessed in the absence of steric and solvent effects from free electron densities. The 1-naphthoxy free electron densities, as calculated from epr spectra,[33] are 0.350 and 0.456 at positions 2 and 4, respectively. On this basis alone, the [**2-AN**]/[**4-AN**] (and [**2-BN**]/[**4-BN**]) ratios are predicted to be $\leq$1. Clearly, this is not the case for [**2-AN**]/[**4-AN**]. In addition, the [**2-BN**]/[**4-BN**] ratios for **1b**, except in *t*-butyl alcohol, are *much* lower than expected. Only the [**2-BN**]/[**4-BN**] ratios for **1a** at 22°C (Table 2) are consistent with the epr-based prediction.

Preferences for addition to 1-naphthoxy that include steric factors, but very small contributions from cage-related inhibitions (including hydrogen-bonding effects available in *t*-butyl alcohol), can be estimated from [**2-AN**]/[**4-AN**] and [**2-BN**]/[**4-BN**] ratios in hexane. The cages afforded by hexane have polarities similar to the polyolefin ones, but *much* weaker walls (so that reactivity of the radical pair is virtually unimpeded by solvent viscosity), and almost no local anisotropy. At 22°C, there is a large disparity between the [**2-AN**]/[**4-AN**] ratios in hexane ($\leq$3) and in the polyolefin films ($\geq$6). By contrast, the [**2-BN**]/[**4-BN**] ratios tend to be somewhat smaller in the polyolefins than in hexane! These completely opposite trends (Table 3), combined with results from irradiation of **BzONa** demonstrate that polyolefin cages interact differently with carbonylated and decarbonylated radical pairs.

Absolute rate constants for phenylacyl/1-naphthoxy radical pair reactions in polyolefinic films

Absolute values of $\mathbf{k_{2A}}$ and $\mathbf{k_{4A}}$ from Eqs. (2) and (3) in the polyolefinic films are 1–2 orders of magnitude slower than in isotropic media of low viscosity[10] (Table 3). Equally notable is the ca. one order of magnitude difference between $\mathbf{k_{2A}}$ and $\mathbf{k_{4A}}$. Due to the complexity of the structures of the five polyolefins, it is not possible to identify one or more of their macroscopic properties that are primarily responsible for the relatively small differences among the $\mathbf{k_{2A}}$ or $\mathbf{k_{4A}}$ values at one temperature. Investigations in a larger number of films with a wide range of crystallinities, branching, etc. will be necessary to determine which aspects of the polymers are most important to cage dynamics of the radical pairs. Regardless, the *breadth* of the $\mathbf{k_{2A}}$ or $\mathbf{k_{4A}}$ values in the polyolefin media at 22°C is small, even when structural differences between **1a** and **1b** are not considered. There is, however, a general trend that both $\mathbf{k_{2A}}$ and $\mathbf{k_{4A}}$ of **1b** decrease by >50% when a film is stretched. Stretching causes similar decreases to $\mathbf{k_{2A}}$ and $\mathbf{k_{4A}}$ for **1a** in **BHDPE** but almost no change is detected in **NDLDPE** for reasons that we do not understand. The general trends of the rate data are consistent with the smaller cages that are caused by film stretching.[17]

The influence of stretching can be discerned also in the activation energies, $Ea_{2\text{-AN}}$ and $Ea_{4\text{-AN}}$, for formation of **2-AN** and **4-AN**, respectively, in unstretched and stretched **NDLDPE** (Table 4). $Ea_{2\text{-AN}}$ and $Ea_{4\text{-AN}}$ have been calculated from the slopes of the Arrhenius plots in Fig. 2; we

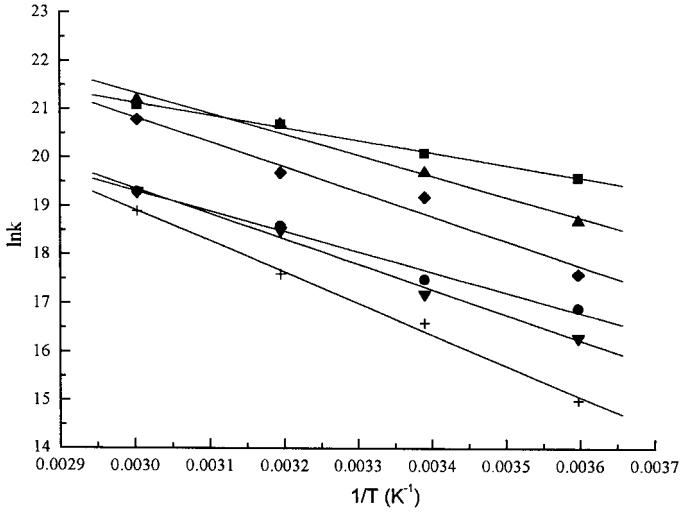

Figure 2. Arrhenius plots of $\mathbf{k_{2A}}$ and $\mathbf{k_{4A}}$ from **1b** in **PE** films: (■) $\mathbf{k_{2A}}$ in **NDLDPE** (u); (●) $\mathbf{k_{4A}}$ in **NDLDPE** (u); (▲) $\mathbf{k_{2A}}$ in **BHDPE** (u); (▼) $\mathbf{k_{4A}}$ in **BHDPE** (u); (◆) $\mathbf{k_{2A}}$ in **NDLDPE** (s); (+) $\mathbf{k_{4A}}$ in **NDLDPE** (s).

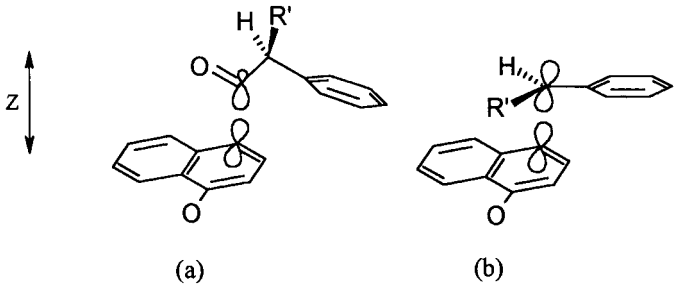

Figure 3. Approximate orientations for radical addition to 1-naphthoxy by (a) carbonylated and (b) decarbonylated radicals from **1a** (R'=H) or **1b** (R'=CH_3). Addition to C-4 is shown. The *z*-axis is orthogonal to the 1-naphthoxy plane.

have less confidence in the preexponential factors, *A*, since they are based on a large extrapolation and are subject to greater error. There is a clear increase in both activation energies when the **NDLDPE** film is stretched. Interestingly, the activation energies in the unstretched film of highest crystallinity, **BHDPE**, are between those in unstretched and stretched **NDLDPE**. The greater crystallinity of **BHDPE** may make the walls of its cages in the amorphous regions stiffer than those of **NDLDPE**.

Influences of polyolefin cages on the fate of singlet biradical pairs from 1

The data presented thus far indicate that macroscopic film properties do not provide important insights into the size, wall stiffness, and anisotropy of the reaction cavities. A similar conclusion was reached from studies of translational diffusion of guest molecules in several polyethylene films.[14] Because the van der Waals volumes of both **1a** (237 Å^3) and **1b** (254 Å^3)[34] are larger than the mean free volumes available in 'voids' of native polyolefin films,[17,35] the occupied cages must be stressed; to some extent, the probe molecules must act as a template to define their own microenvironments. From positron annihilation studies, the average void volumes are 139 and 121 Å^3 for unstretched and stretched **NDLDPE**, respectively, and 124 and 113 Å^3 for unstretched and stretched **BHDPE**, respectively.[17] Guest molecules of **1** feel external pressures from neighboring polymer chains that increase upon film stretching. In addition to reducing the available volume in a cage, macroscopically stretching a film may induce other microscopic changes by increasing wall stiffness and altering cage shapes.[5]

The orientations of approach taken by an acyl and a benzylic radical when adding to a π-orbital of a 1-naphthoxy ring are different (Fig. 3). Orbital overlap during bond formation requires that the long axis of *bent* acyl[36] be projected obliquely and planar benzylic be projected approximately coparallel to the plane of 1-naphthoxy. Consequently, the shape changes of a cage during transformation of a molecule of **1** to a keto precursor of **AN** or **BN** must differ. The ability of either type of keto intermediate to form will be subject to constraints imposed by the rates of relaxation of the molecules in isotropic media or chains in polymeric media that define the cage walls. Those rates are very rapid in isotropic media of low viscosity. However, they are slower than or comparable to the time scales for in-cage radical-pair recombinations in polyolefinic media.[27] Consequently, the polymeric cages will resist the creation of additional space in the dimension orthogonal to the naphthoxy plane (*z*-axis). Because formation of **AN** keto precursors requires creation of more space along this axis than do the **BN** precursors, the rates of the former should be more affected by the polyolefinic cages. Thus, a probable source of the greater photoproduct selectivity and rate diversity among **AN** isomers (N.B., $\mathbf{k_{2A}} \geq 6\mathbf{k_{4A}}$) is 'viscous space' (i.e. spatial contraints imposed *anisotropically* by the media) rather than steric or electronic factors intrinsic to the reacting species.[37]

Conclusions and general considerations

We have demonstrated that a wide variety of polyolefin media influence in very similar ways the dynamics and fates of singlet radical pairs generated by irradiation of two 1-naphthyl phenylacylates with similar shapes and molecular volumes. Evidence has been presented for the amorphous regions of the polymer films being the major locus of reactive cages. Although the polyolefinic media are morphologically diverse, the reaction cavities they provide to molecules of **1** appear to be quite similar. This is probably a result of both the similar shapes of the esters and the saturated hydrocarbon-like nature of the media chains. The cages are not just viscous analogues of liquid hydrocarbons since the shapes of the guest molecules appear to mandate the types of motions available to their radical pairs: wall stiffness (which in this case is related to relaxation rates of the polyolefinic chains) and cage shape anisotropy force the radical pairs to retain some memory of their precursor; the esters act as partial templates for the space that can be explored by the radical pairs they produce. As a result, the lifetimes of the initial phenylacyl/1-naphthoxy radical pairs are lengthened significantly, allowing some decarbonylation to occur in-cage at temperatures where it is not observed in non-viscous, isotropic media. Additionally, the benzylic/1-naphthoxy radical pairs resulting from decarbonylation are able to explore a larger space and nearly 'equilibrate' before combining.

Of equal importance is our demonstration that absolute rate constants for radical-pair recombination processes can be measured in polyolefin media without direct observation of the radicals. Regardless of the detailed reasons for the substrate dependence on the rate constants, the method described for calculating them should be applicable to other isotropic and anisotropic media *provided they are capable of trapping radicals that escape from the initial cages*. Additionally, the time frame in which the decarbonylation clock operates can be varied by more

than 15 orders of magnitude by changing the structure of the acyl radical[13,38] Judicious choice of the acyl portion of the reactant will allow a wide variety of molecular motions of radical pairs to be investigated quantitatively. Clearly, several unexpected trends in radical-pair reactivity have been discovered, and much more mechanistic information should be available from future experiments.

Experimental

Instrumentation

Melting points are corrected. IR spectra (in Nujol mulls or KBr pellets) were recorded on a MIDAC FT-IR or NICOLET 7000 series FT-IR spectrometer. ^{1}H NMR spectra were obtained on Bruker 270 MHz NMR spectrometer with a Tecmag operating system or Varian Mercury 300 MHz NMR spectrometer interfaced to a Sun SparcStation 5. UV–VIS absorption spectra were recorded on Perkin–Elmer Lambda 6 UV/VIS spectrophotometer. Fluorescence decay histograms were obtained with an Edinburgh Analytical Instruments model FL900 single photon counting instrument using H_2 as the lamp gas. Solutions and films were degassed in 4 mm thick quartz cuvettes on an Hg-free vacuum line using several freeze–pump–thaw cycles at $<10^{-5}$ Torr. 'Scatter' peaks of very short duration present in the decay profiles of the polymer films were included in the fitting analyses but are not reported.

Gas chromatography (GC) was conducted on a Hewlett-Packard 5890 gas chromatograph equipped with a flame ionization detector, a Hewlett-Packard 3393A integrator, and either a 2.0 μm Hewlett Packard HP-17 (10 m×0.53 mm or 5 m×0.53 mm) or 0.25 μm Alltech DB-5 (15 m×0.25 mm) column. GC–MS was performed on a FISONS MD-800 GC–MS instrument using a DB-5 column.

HPLC analyses used a Waters 440 absorbance detector (254 nm) and a Waters 6000A solvent delivery system and either an Alltech 5 μ silica gel (250 mm×4.4 mm) column (15:1:1 (v:v:v) hexanes/ethyl acetate/methanol) or a Waters Symmetry C18 column (3.9 mm×150 mm) (2:1 (v:v) acetonitrile/water).

Reagents

Styrene (inhibited with 10–15 ppm 4-*tert*-butylcatechol, 99+%) and benzopinacol (99%) were used as received from Aldrich. Benzhydrol (Aldrich, 99%) was recrystallized from petroleum ether. Benzophenone (Aldrich, 99%) was recrystallized from benzene. Hexane (Aldrich, 99+%) and *t*-butyl alcohol (Fisher, 99%) were distilled before use when a solvent for photoreactions. Thiophenol (ACROS) was 99% by GC analysis after distillation under N_2 (just before use). 1-Naphthol, a dark red solid (Aldrich, 99+%), was chromatographed (silica gel, 5% ethyl acetate in hexane) to yield white needles, mp 93.7–95.4°C (lit.[39] mp 95.8–96.0°C). Methylene chloride was dried over P_2O_5, distilled, and then stored over 4 Å molecular sieves. THF was dried and distilled from Na/benzophenone.[40]

High density polyethylene films (**BHDPE**; 51% crystallinity, type ES-300; Polialden Petroquimica, Brasil) and low density polyethylene films (**NDLDPE**; 26% crystallinity; DuPont of Canada) have been characterized previously.[14,17,41] Linear low density polyethylene films (**LLDPE**; thickness, 25 μm; density, 0.917 g/cm^3, 21% crystallinity based upon DSC[42]) was from Exxon. The **PE** films were immersed in 3 chloroform aliquots during one week to remove additives and dried. Granules of isotactic polypropylene (*iso*-**PPP**; ca. 39% crystalline from DSC[43]; Slovnaft, Slovakia) and syndiotactic polypropylene (*syn*-**PPP**; heat of melting=28 J/g from DSC, but no reliable heat of melting for 100% crystalline material is available;[15] M_w 1.6×10^4, M_w/M_n 2.2, R-M-M-R/total sequences=1.27% by NMR; Himont, Ferrara, Italy) were pressed into films (260 μm thick) at 35–40 K Newtons pressure for 2 min at 190 and 180°C, respectively. They were immersed in three cyclohexane aliquots over a period of at least one week to remove antioxidants and plasticizers and then dried under vacuum. All of the leached films were stored under a nitrogen atmosphere in the dark until use. Strips of film were immersed in methylene chloride (**PE**) or cyclohexane (**PPP**) solutions containing 10–20 mM **1** for various periods to achieve the desired dopant concentrations. Then the film surfaces were rubbed gently with a tissue soaked in hexane and dried under a stream of nitrogen before irradiation. Concentrations of **1** in films were calculated from averaged optical densities of at least three different parts of each film, film thicknesses, and molar extinction coefficients (ϵ) of the dopant molecule in hexane (at 280 nm). Some doped films were cold-stretched slowly by hand to ca. 4 (**NDLDPE**) or 5 (**LLDPE** and **BHDPE**) times their original length.

Irradiation procedures

Films were placed in closed Pyrex glass containers, purged with nitrogen for about 15 min, and irradiated on both faces for the same length of time with the Pyrex-water filtered output of a Hanovia 450 W medium pressure lamp. At temperatures other than 22°C, films in nitrogen-filled Pyrex tubes were irradiated in a stirred (heated or cooled) water bath whose temperature was constant (±1°C) during the exposure period. Nitrogen was bubbled through solutions in hexane and *t*-butyl alcohol for ca. 15 min prior to irradiation under nitrogen in closed Pyrex tubes.

Product analyses

Irradiated films were kept in the dark in methylene chloride (**PE**) or cyclohexane (**PPP**) that were changed every 6 h until no starting material and/or photoproducts were detectable by HPLC and/or GC analyses in the last aliquot. The combined aliquots were concentrated under reduced pressure before being analyzed. Photoproducts were identified and quantified using authentic samples and GC analyses and by their fragmentation patterns during GC–MS analyses. Irradiated solutions in hexane and *t*-butyl alcohol were analyzed directly by GC.

Benzophenone sensitized photoreactions of 1a[36,44]

Nitrogen-saturated hexane solutions of benzophenone (3.0 mM)/benzhydrol (6.0 mM) and benzophenone

(3.0 mM)/benzhydrol (6.0 mM)/**1a** (6.0 mM) were irradiated side-by-side in closed Pyrex tubes using an extra 0–52 glass filter (cutoff <340 nm). UV spectra and reverse phase HPLC chromatograms were recorded before and after irradiations. Changes in the concentration of benzophenone were monitored at 360 nm.

Thiol-trapping experiment

Different amounts of thiophenol were added to Pyrex tubes containing 2 mL aliquots of N_2-saturated 2 mM **1a** in hexane. The solutions were irradiated side-by-side for the same period and analyzed by GC.

Syntheses

Spectroscopic data for some of the previously reported compounds are available in Appendix A.

1-Naphthyl phenylacetate (1a) was synthesized in 80% yield from phenylacetic acid and 1-naphthol:[45] >99% pure by normal phase HPLC and GC, mp 43.0–45.3°C (lit. mp[46] 46–47°C).

Benzyl 1-naphthyl ether was synthesized in 74% yield from 1-naphthol and benzyl bromide:[47] >99% by GC, mp 72.5–75.0°C (lit. mp[47] 77°C).

2-Phenylacetyl-1-naphthol and 4-phenylacetyl-1-naphthol were synthesized from **1a** and $AlCl_3$ in CS_2.[48] The crude product, a red oil, was chromatographed (silica gel) with 2% ethyl acetate in hexanes to elute first 2-phenylacetyl-1-naphthol, a bright yellow solid (1.2 g, 46%), mp 90.7–93.5°C (lit. mp[49] 96°C). $CHCl_3$ then eluted 4-phenylacetyl-1-naphthol, a yellow solid (0.5 g, 23%), mp 181.8–184.5°C (lit. mp[49,50] 185–187°C).

2-Benzyl-1-naphthol was prepared by zinc amalgam reduction[51] of 2-benzoyl-1-naphthol (mp 59.8–68.7°C)[52] in 7% yield: pale yellow needles, mp 68.7–72.6°C (lit. mp[53] 73–7°C).

4-Benzyl-1-naphthol was synthesized by zinc amalgam reduction[51] of 4-benzoyl-1-naphthol (mp 156.6–161.1°C[54] in 3% yield: off-white solid, mp 119.5–123.0°C (lit. mp[55] 125–126°C).

1-Benzylnaphthalene was prepared by hydrazine/KOH reduction of 1-benzoylnaphthalene (mp 72.4–75.5°C)[56] in 45% yield: white solid, 98% pure by reversed phase **HPLC**, mp 57.1–59.5°C (lit. mp[57] 57–58°C).

1-Naphthyl 2-phenylpropanoate (1b) was prepared from purified 1-naphthol and 2-phenylpropanoic acid[45] in 73% yield: white needle crystals, >99% by GC, mp 51.2–53.3°C (lit. mp[58] 49–50°C).

1-(1-Naphthyl)-1-phenylethane. Under a nitrogen atmosphere, a stirred solution of 1-(1-naphthyl)-1-phenylethanol (0.9 g, 3.6 mmol), $NaBH_4$ (1.5 g, 35 mmol), and 20 mL dry THF was cooled in an ice-bath and 20 mL trifluoroacetic acid (TFA) was added during about 1 h. (*Note: The addition of TFA must be extremely slow to avoid uncontrolled gas evolution.*) The reaction mixture was poured into a stirred solution of 30 mL 25% aqueous NaOH that was pre-cooled in an ice-bath. It was extracted with ether (3×30 mL) and the combined etherates were washed with a copious amount of water and dried (Na_2SO_4). The yellowish oil from evaporation of the liquid was chromatographed (silica gel; hexanes) to yield 0.7 g (83%; >98% by GC) of a colorless oil that became a white solid upon refrigeration: mp 58–62°C (lit. mp[59] 62–3°C).

2-(1-Phenylethyl)-1-naphthol and 4-(1-phenylethyl)-1-naphthol. Styrene (1.1 mL, 10 mmol) in 4 mL toluene was added periodically during a 2 h period to a solution of 1-naphthol (3.0 g, 21 mmol), 10 mL toluene, and 3 drops of conc sulfuric acid. After 1 h, the liquid was evaporated to yield a dark red oil that was chromatographed twice (silica gel; 2% ethyl acetate in hexanes) to yield 0.4 g (16%; >96% pure by reverse phase HPLC) 2-(1-phenylethyl)-1-naphthol as a pale red oil. IR (neat) 3514 (b and s, –OH), 3025 and 3058 cm^{-1} (aromatic); ^1H NMR ($CDCl_3$/TMS, 300 MHz) 7.19–8.10 (m, 11H, aromatic), 5.10 (s, 1H, –OH), 4.49 (quartet, 1H, –C(O)–CH(CH_3)Ph, J=7.2 Hz), 1.74 ppm (d, 3H, –C(O)–CH(CH_3)Ph, J=7.2 Hz); UV/Vis (2/1 acetonitrile/water) λ_{max} (ϵ) 293 (4210); mass m/z calculated for $C_{18}H_{16}O$ 248, found 248.

4-(1-Phenylethyl)-1-naphthol and 1-naphthol eluted together and were separated by reverse phase column chromatography (C18-functionalized silica gel; 1:1 (v:v) methanol:water (1-naphthol) followed by 9:1 (v:v) methanol:water (4-(1-phenylethyl)-1-naphthol)). The former was a red oil, 0.25 g (10%; >95% by reverse phase HPLC). IR (neat) 3541 (b and s, –OH), 3026 and 3059 cm^{-1} (aromatic); ^1H NMR ($CDCl_3$/TMS, 300 MHz) 6.77–8.24 (m, 11H, aromatic), 5.81 (s, 1H, –OH), 4.80 (quartet, 1H, –C(O)–CH(CH_3)Ph, J=6.9 Hz), 1.72 ppm (d, 3H, –C(O)–CH(CH_3)Ph, J=6.9 Hz); UV/Vis (2/1 acetonitrile/water) λ_{max} (ϵ) 303 (6150); mass m/z calculated for $C_{18}H_{16}O$ 248, found 248.

1-[2-(1-Hydroxynaphthyl)]-2-phenyl-1-propanone and 1-[4-(1-hydroxynaphthyl)]-2-phenyl-1-propanone. A mixture of $AlCl_3$ (1.0 g, 7.5 mmol), **1b** (1.65 g, 6 mmol), and 30 mL CS_2 was refluxed overnight in a dry atmosphere. The residue, after evaporation of the liquid, was treated with 20 mL 17% hydrochloric acid and extracted with ether (3×50 mL). The combined ether layers were washed with water (3×50 mL), dried (Na_2SO_4), and evaporated to a red oil which was chromatographed (silica gel, 3% ethyl acetate in hexanes) to yield 0.55 g (33%; >98% by GC) 1-[2-(1-hydroxynaphthyl)]-2-phenyl-1-propanone as a yellow oil. IR (neat) 3300 (b and s, –OH), 3028, 3062 (aromatic), 1622 cm^{-1} (s, C=O); ^1H NMR ($CDCl_3$/TMS, 300 MHz) 14.19 (s, 1H, –OH), 7.10–8.42 (m, 11H, aromatic), 4.75 (quartet, 1H, CH(CH_3)Ph, J=6.9 Hz), 1.57 ppm (d, 3H, CH(CH_3)Ph, J=6.9 Hz); UV/Vis (2/1 acetonitrile/water) λ_{max} (ϵ) 265 (39000), 371 (8290); mass m/z calculated for $C_{19}H_{16}O_2$ 276, found 276. Further elution (chloroform) yielded 0.1 g (6%;>97% by GC) 1-[4-(1-hydroxynaphthyl)]-2-phenyl-1-propanone as a yellow oil. IR (Nujol) 3175 (b and s, –OH), 1639 cm^{-1} (s, C=O); ^1H NMR ($CDCl_3$/TMS, 300 MHz) 6.71–8.70 (m, 11H, aromatic), 6.30 (s, 1H, –OH), 4.72 (quartet, 1H,

$CH(CH_3)Ph$, J=6.9 Hz), 1.57 ppm (d, 3H, $CH(CH_3)Ph$, J=6.9 Hz); UV/Vis (2/1 acetonitrile/water) λ_{max} (ϵ) 238 (28900), 325 (10200); mass m/z calculated for $C_{19}H_{16}O_2$ 276, found 276.

(α-Methyl)benzyl 1-naphthyl ether. A mixture of 1-naphthol (2.0 g, 14 mmol), (1-bromoethyl)benzene (2.0 mL, 15 mmol), K_2CO_3 (10 g), and 60 mL acetone were refluxed overnight and the liquid was evaporated to a residue that was taken in ether (3×50 mL). The ether was washed with water (2×50 mL), 8% aqueous NaOH (2×50 mL) and a copious amount of water, and dried (Na_2SO_4). A reddish oil, after evaporation of ether, was eluted (silica gel; 3% ethyl acetate in hexanes) to yield a colorless oil. Recrystallization from hexane gave 2.0 g (59%; >99% by GC) of white crystals, mp 67.0–68.4°C. IR (KBr) 3055, 3026 (w, aromatic), 1099, 1267 cm^{-1} (C–O); ^1H NMR ($CDCl_3$/TMS, 300 MHz) 6.66–8.46 (m, 12H, aromatic), 5.54 (quartet, 1H, $-OCH(CH_3)Ph$, J=6.3 Hz), 1.76 ppm (d, 3H, $-OCH(CH_3)Ph$, J=6.3 Hz); mass m/z calculated for $C_{18}H_{16}O$ 248, found 248.

1-(1-Naphthyl)-1-phenylethanol. Under dry atmosphere, 1.5 mL CH_3MgBr (3 M solution in ether, 4.5 mmol) was added dropwise during 30 min to a stirred, cooled (0°C) solution of 1-benzoylnaphthalene (0.96 g, 4 mmol) and 20 mL anhydrous Et_2O. After 5 h, an additional 1.2 mL CH_3MgBr (3 M solution in ether, 3.6 mmol) was added and the stirring was continued overnight at room temperature. 30 mL 20% Aqueous NH_4Cl solution and 30 g ice were added and the mixture was extracted with ether (3×30 mL). The combined etherates were washed with saturated $NaHCO_3$ and a copious amount of water, and dried (Na_2SO_4). Evaporation of the liquid yielded 0.9 g (91%; one spot by TLC) of a pale yellow oil. IR (neat) 3564 and 3452 cm^{-1} (s and b, OH); ^1H NMR ($CDCl_3$/TMS, 300 MHz) 7.20–7.90 (m, 12H, aromatic), 2.42 ppm (s, 1H, $C(OH)CH_3NpPh$), 2.08 (s, 3H, $C(OH)CH_3NpPh$).

Acknowledgements

We are grateful to the National Science Foundation for its support of this research. Dr Jon Baldvins of Waters Associates, Dr Jawad Naciri and Mr Chip Patterson of the Naval Research Laboratory, and Dr David Abdallah are thanked for their help with HPLC analyses. Mr Mario Lutterotti of Dupont of Canada and Ms Nancy Richter of Exxon Chemical Company are thanked for kindly supplying some of the polymer films and technical information about them.

Appendix A

^1H NMR, IR, UV/Vis, and mass spectral data for some of the previously reported compounds synthesized for this project.

Spectral data for previously reported compounds:

1-Naphthyl phenylacetate (1a). IR (KBr) 3055 (w, aromatic), 1748 cm^{-1} (s, C=O); ^1H NMR ($CDCl_3$/TMS, 270 MHz) 7.21–7.85 (m, 11H, aromatic), 4.02 ppm (s, 2H, $-OCH_2$); UV/Vis (hexane) λ_{max} (ϵ) 280 (7000), λ_{sh} (ϵ) 313 (340); mass m/z calculated for $C_{18}H_{14}O_2$ 262, found 262.

Benzyl 1-naphthyl ether. IR (KBr) 3055, 3033 (w, aromatic), 1095, 1268 cm^{-1} (C–O); ^1H NMR ($CDCl_3$/TMS, 300 MHz) 6.89–8.39 (m, 11H, aromatic), 5.27 ppm (s, 2H, $-OCH_2$); mass m/z calculated for $C_{17}H_{14}O$ 234, found 234.

2-Phenylacetyl-1-naphthol. IR (KBr) 3414, 3476 (s and b, –OH), 3057 (w, aromatic), 1618 cm^{-1} (s, C=O); ^1H NMR ($CDCl_3$/TMS, 300 MHz) 13.98 (s, –OH), 7.25–8.47 (m, 11H, aromatic), 4.38 ppm (s, 2H, $-CH_2$); UV/Vis (2/1 acetonitrile/water) λ_{max} (ϵ) 262 (34200), 370 (7060); mass m/z calculated for $C_{18}H_{14}O_2$ 262, found 262.

4-Phenylacetyl-1-naphthol. IR (KBr) 3414, 3287 (s and b, –OH), 3027, 3061 (w, aromatic), 1655 cm^{-1} (C=O); ^1H NMR ($CDCl_3$/TMS, 270 MHz) 8.91 (d, 1H, J=7.91 Hz, aromatic), 8.24 (d, 1H, J=7.03 Hz, aromatic), 8.00 (d, 1H, J=8.79 Hz, aromatic), 7.58 (m, 2H, aromatic), 7.30 (m, 4H, aromatic), 6.78 (d, 2H, J=7.91 Hz, aromatic), 6.14 (s, 1H, –OH), 4.36 ppm (s, 2H, $-CH_2$); UV/Vis (2/1 acetonitrile/water) λ_{max} (ϵ) 238 (29500), 326 (11600); mass m/z calculated for $C_{18}H_{14}O_2$ 262, found 262.

2-Benzyl-1-naphthol. IR (KBr) 3449 cm^{-1} (s and b, –OH); ^1H NMR ($CDCl_3$/TMS, 270 MHz) 7.23–8.11 (m, 11H, aromatic), 5.13 (s, 1H, –OH), 4.17 ppm (s, 2H, $-CH_2$). When a drop of D_2O was added to the NMR tube and it was shaken thoroughly, the peak at 5.13 ppm moved to 4.70 ppm (probably HDO); UV/Vis (2/1 acetonitrile/water) λ_{max} (ϵ) 292 (4200); mass m/z calculated for $C_{17}H_{14}O$ 234, found 234.

4-Benzyl-1-naphthol. IR (KBr) 3405 cm^{-1} (s and b, –OH); ^1H NMR ($CDCl_3$/TMS, 270 MHz) 6.75–8.24 (m, 11H, aromatic), 5.19 (s, 1H, –OH), 4.37 ppm (s, 2H, $-CH_2$). When a drop of D_2O was added to the NMR tube and it was shaken thoroughly, the peak at 5.19 ppm moved to 4.70 ppm (probably HDO). UV/Vis (2/1 acetonitrile/water) λ_{max} (ϵ) 303 (6900); mass m/z calculated for $C_{17}H_{14}O$ 234, found 234.

1-Benzylnaphthalene. IR (KBr) 3079, 3063, 3047, 3021 cm^{-1} (w, aromatic); ^1H NMR ($CDCl_3$/TMS, 300 MHz) 4.46 (s, 2H, $-CH_2$), 7.18–7.49 (m, 9H, aromatic), 7.75–8.01 ppm (m, 3H, aromatic); mass m/z calculated for $C_{17}H_{14}$ 218, found 218.

1-Naphthyl 2-phenylpropanoate (1b). IR (Nujol) 3029, 3061 (w, aromatic), 1752 (s, C=O), 1135 cm^{-1} (C–O); ^1H NMR ($CDCl_3$/TMS, 300 MHz) 7.15–7.86 (m, 12H, aromatic), 4.18 (quartet, 1H, $-C(O)-CH(CH_3)Ph$, J= 6.9 Hz), 1.76 ppm (d, 3H, $-C(O)-CH(CH_3)Ph$, J= 6.9 Hz); UV/Vis (hexane) λ_{max} (ϵ) 280 (7100), λ_{sh} (ϵ) 313 (330); mass m/z calculated for $C_{19}H_{16}O_2$ 276, found 276.

1-(1-Naphthyl)-1-phenylethane. IR (KBr) 3019, 3060, 3080 and 1596 cm^{-1} (w, aromatic); ^1H NMR ($CDCl_3$/TMS, 300 MHz) 7.13–8.06 (m, 12H, aromatic), 4.93 (q,

1H, J=7.2 Hz, $CHCH_3$NpPh), 1.76 ppm (d, 3H, J=7.2 Hz, $CHCH_3$NpPh); mass m/z calculated for $C_{18}H_{16}$ 232, found 232.

References

1. (a) Weiss, R. G.; Ramamurthy, V.; Hammond, G. S. *Acc. Chem. Res.* **1993**, *26*, 530. (b) Ramamurthy, V.; Weiss, R. G.; Hammond, G. S. In *Advances in Photochemistry*; Volman, D. H., Neckers, D., Hammond, G. S., Eds.; Wiley-Interscience: New York, 1993; Vol. 18, p 67.
2. (a) Cui, C.; Naciri, J.; He, Z.; Costantino, R. M.; Lu, L.; Hammond, G. S.; Weiss, R. G. *Quimica Nova* **1993**, *16*, 578. (b) Naciri, J.; He, Z.; Costantino, R. M.; Lu, L.; Hammond, G. S.; Weiss, R. G. In *Multidimensional Spectroscopy of Polymers*; Urban, M. W., Provder, T., Eds.; American Chemical Society: Washington, 1995; Chapter 25.
3. Franck, J.; Rabinowitch, E. *Trans. Faraday Soc.* **1934**, *30*, 120 and subsequent papers in the series.
4. See for instance: (a) Fletcher, B.; Suleman, N. K.; Tanko, J. M. *J. Am. Chem. Soc.* **1998**, *120*, 11839. (b) Male, J. L.; Lindfors, B. E.; Covert, K. J.; Tyler, D. R. *J. Am. Chem. Soc.* **1998**, *120*, 13176. (c) Koenig, T. W.; Hay, B. P.; Finke, R. G. *Polyhedron* **1988**, *7*, 1499.
5. Cui, C.; Weiss, R. G. *J. Am. Chem. Soc.* **1993**, *115*, 9820.
6. (a) Griller, D.; Ingold, K. U. *Acc. Chem. Res.* **1980**, *13*, 317. (b) Pincock, J. A. *Acc. Chem. Res.* **1997**, *30*, 43.
7. (a) Nevill, S. M.; Pincock, J. A. *Can. J. Chem.* **1997**, *75*, 232. (b) Horner, J. H.; Tanaka, N.; Newcomb, M. *J. Am. Chem. Soc.* **1998**, *120*, 10379 and refs cited therein.
8. (a) Martin-Esker, A. A.; Johnson, C. C.; Horner, J. H.; Newcomb, M. *J. Am. Chem. Soc.* **1994**, *116*, 9174. (b) Newcomb, M.; Manek, M. B.; Glenn, A. G. *J. Am. Chem. Soc.* **1991**, *113*, 949.
9. See for instance: (a) Bowry, V. W.; Ingold, K. U. *J. Am. Chem. Soc.* **1991**, *113*, 5699. (b) Liu, K. E.; Johnson, C. C.; Newcomb, M.; Lippard, S. J. *J. Am. Chem. Soc.* **1993**, *115*, 939. (c) DeCosta, D. P.; Pincock, J. A. *J. Am. Chem. Soc.* **1993**, *115*, 2180. (d) Nagahara, K.; Ryu, I.; Kambe, N.; Komatsu, M.; Sonoda, N. *J. Org. Chem.* **1995**, *60*, 7384.
10. Nakagaki, R.; Hiramatsu, M.; Watanabe, T.; Tanimoto, Y. *J. Phys. Chem.* **1985**, *89*, 3222.
11. A different approach by Garcia-Garibay and coworkers[a] employs photoreactions in neat crystalline phases. It has the advantage that molecular conformations are known with greater certainty than in viscous media, but it has the disadvantage that the range of motions available to the reactive species is severely limited. Also, the use of precursors to triplet radical pairs, to time much slower events than the ones of interest here, is well-established.[b,c] (a) Choi, T.; Peterfy, K.; Khan, S. I.; Garcia-Gariby, M. A. *J. Am. Chem. Soc.* **1996**, *118*, 12477. (b) Hrovat, D. A; Liu, J. H.; Turro, N. J.; Weiss, R. G. *J. Am. Chem. Soc.* **1984**, *106*, 5291. (c) Cozens, F. L.; Scaiano, J. C. *J. Am. Chem. Soc.* **1993**, *115*, 5204.
12. Gu, W.; Warrier, M.; Ramamurthy, V.; Weiss, R. G. *J. Am. Chem. Soc.* **1999**, *121*, 9467.
13. Turro, N. J.; Gould, I. R.; Baretz, B. H. *J. Phys. Chem.* **1983**, *87*, 531.
14. Zimerman, O. E.; Cui, C.; Wang, X.; Atvars, T.; Weiss, R. G. *Polymer* **1998**, *39*, 1177.
15. (a) Uedono, A.; Kawano, T.; Tanigawa, S.; Ban, M.; Kyoto, M.; Uozumi, T. *J. Polym. Sci. B: Polym. Phys.* **1997**, *35*, 1601 and references cited therein. (b) Bu, H.; Cheng, S. Z. D.; Wunderlich, B. *Makromol. Chem. Rapid Commun.* **1988**, *9*, 75. (c) Brandrup, J.; Immegut, E. H.; Grulke, E. A. *Polymer Handbook*, 4th ed.; Wiley: New York, 1999; V/21.
16. Talhavini, M.; Atvars, T. D. Z.; Cui, C.; Weiss, R. G. *Polymer* **1996**, *37*, 4365.
17. Gu, W.; Hill, A. J.; Wang, X.; Cui, C.; Weiss, R. G. *Macromolecules*, submitted for publication.
18. (a) Zavitsas, A. A.; Chatgilialuglu, C. *J. Am. Chem. Soc.* **1995**, *117*, 10645. (b) Franz, J. A.; Alnajjar, M. S.; Barrows, R. D.; Kaisaki, D. L.; Camaioni, D. M.; Suleman, N. K. *J. Org. Chem.* **1986**, *51*, 1446.
19. Moore, W. M.; Hammond, G. S.; Foss, R. P. *J. Am. Chem. Soc.* **1961**, *83*, 2789.
20. Leigh, W.; Arnold, D. R. *J. Chem. Soc., Chem. Commun.* **1980**, 406.
21. Bellus, D. *Adv. Photochem.* **1971**, *8*, 109 (and references cited therein).
22. Meranda, M. A. *Handbook of Organic Photochemistry and Photobiology*; Horspool, W. M., Song, P.-S., Eds.; CRC: Boca Raton, 1995; Chapter 47.
23. Sternberg, V. I. *Organic Photochemistry*; Chapman, O. L., Ed.; Arnold: New York, 1967.
24. Gritsan, N. P.; Tsentalovich, Y. P.; Yurkovskaya, A. V.; Sagdeev, R. Z. *J. Phys. Chem.* **1996**, *100*, 4448.
25. **BzN**, from decarboxylation, is also present in small yields.[a,b] Since $\mathbf{k_1}$ occurs in parallel with lysis ($\mathbf{k_c}$), the extent of decarboxylation does not influence the ratios of the relative yields of the photoproducts derived from the radical pairs. (a) Finnegan, R. A.; Knutson, D. *J. Am Chem. Soc.* **1967**, *89*, 1971. (b) Finnegan, R. A.; Knutson, D. *Chem. Ind.* **1965**, 1837.
26. Jent, F.; Paul, H.; Roduner, E.; Heming, M.; Fischer, H. *Int. J. Chem. Kinet.* **1986**, *18*, 1113.
27. The relaxation times of occupied sites in polyolefins are difficult to estimate because the size and shape of each guest will influence the chain segments constituting its host cage differently. However, the NMR determined correlation time of C–H dipolar interactions in the amorphous regions of polyethylene[a] and polypropylene[b] are $\leq$50 ns. The correlation time of pyrene, which is expected to disturb its cage environment much more than molecules of **1**, is ca. two order of magnitude shorter than that of its host, an ethylene–propylene rubber.[a] (a) Tai, Y.; Okazaki, M.; Toriyami, K. *J. Chem. Soc., Faraday Trans.* **1992**, *88*, 23. (b) Tanaka, H.; Inoue, Y. *Eur. Polym. J.* **1993**, *29*, 569.
28. Gu, W.; Warrier, M.; Schoon, B.; Ramamurthy, V.; Weiss, R. G. *Langmuir*, accepted for publication.
29. Tsentalovich, Y. P.; Fischer, H. *J. Chem. Soc., Perkin Trans. 2* **1994**, 729.
30. Braun, W.; Rajbenbach, L.; Eirich, F. R. *J. Phys. Chem.* **1962**, *66*, 1591.
31. (a) Michaels, A. S.; Bixler, H. J. *J. Polym. Sci.* **1961**, *50*, 413. (b) Birks, J. B. In *Organic Molecular Photophysics*; Birks, J. B., Ed.; Wiley: New York, 1973; Vol. 1, p 403.
32. (a) Phillips, P. J. *Chem. Rev.* **1990**, *90*, 425. (b) Jang, Y. T.; Phillips, P. J.; Thulstrup, E. W. *Chem. Phys. Lett.* **1982**, *93*, 66. (c) Meirovitch, E. *J. Phys. Chem.* **1984**, *88*, 2629. (d) Naciri, J.; Weiss, R. G. *Macromolecules* **1989**, *22*, 3928. (e) He, Z; Hammond, G. S.; Weiss, R. G. *Macromolecules* **1992**, *25*, 1568. (f) Jenkins, R. M.; Hammond, G. S.; Weiss, R. G. *J. Phys. Chem.* **1992**, *96*, 496.
33. (a) Dixon, W. T.; Foster, W. E. J.; Murphy, D. *J. Chem. Soc., Perkin II* **1973**, *15*, 2124. (b) Karplus, M.; Fraenkel, G. K. *J. Chem. Phys.* **1961**, *35*, 1312.
34. Bondi, A. *J. Phys. Chem.* **1964**, *68*, 441.
35. (a) Jean, Y. C.; Deng, Q. *J. Polym. Sci. B, Polym. Phys.* **1992**,

30, 1359. (b) Serna, C.; Abbe, J. Ch.; Duplatre, G. *Phys. Status Solidi A* **1989**, *115*, 389.
36. Cui, C.; Wang, X.; Weiss, R. G. *J. Org. Chem.* **1996**, *61*, 962.
37. The marginally larger $\mathbf{k_{2A}}$ (or $\mathbf{k_{4A}}$) for **1b** than **1a** in a common polymer medium may be attributed to different ground state conformations,[17,36] or to the somewhat greater directional compression exerted by the cages on the radical pairs as a result of their slightly different sizes and the orientational factors discussed in the text. Probes with a range of van der Waals volumes much larger than provided by **1a** and **1b** or different cavity sizes with one probe[a] will be necessary to test these hypotheses properly. (a) Wang, C. L.; Hirade, T.; Maurer, F. H. J.; Eldrup, M.; Pedersen, N. J. *Polymer* **1998**, *108*, 4654.
38. Lunazzi, L.; Ingold, K. U.; Scaiano, J. C. *J. Phys. Chem.* **1983**, *87*, 529 (and references cited therein).
39. May, O. E.; Berliner, J. F. T.; Lynch, D. F. *J. Am. Chem. Soc.* **1927**, *49*, 1012.
40. Perrin, D. D.; Armarego, W. L. F. Purification of Laboratory Chemicals. *3rd* **1988**, 284.
41. Some of the crystallinities have been have been recalculated from the values reported in Ref. 14.
42. Gray, A. P. *Thermochim. Acta* **1970**, *1*, 563.
43. Wunderlich, B. *Macromolecular Physics, Crystal Melting*; Academic: New York, 1980; Vol. 3.
44. Moore, W. M.; Ketchum, M. *J. Am. Chem. Soc.* **1962**, *84*, 1368.
45. Moore, J. S.; Stupp, S. I. *Macromolecules* **1990**, *23*, 65.
46. Chu, E. J.-H.; Shen, Z.-I.; Chie, T.-L.; Tuan, T. S. *J. Am. Chem. Soc.* **1944**, *66*, 653.
47. Dermer, V. H.; Dermer, O. C. *J. Org. Chem.* **1939**, *3*, 289.
48. Furniss, B. S.; Hannaford, A. J.; Smith, P. W. G.; Tatchell, A. R. *Vogel's Textbook of Practical Organic Chemistry*, 5th ed; Wiley: New York, 1989.
49. Cheema, U. S.; Venkataraman, K. *J. Chem. Soc.* **1932**, 918.
50. Buu-Hoi, Ng. Ph.; Lavit, D. *J. Org. Chem.* **1955**, *20*, 823.
51. Furniss, B. S.; Hannaford, A. J.; Smith, P. W. G.; Tatchell, A. R. *Vogel's Textbook of Practical Organic Chemistry*, 5th ed.; Wiley: New York, 1989; p 467.
52. Anderson, L. C.; Thomas, D. G. *Chem. Soc.* **1943**, *65*, 234.
53. Aly, A. A.; Fahmy, A. M.; Atalla, A. A. *Ind. J. Chem. B* **1994**, *33*, 139.
54. Schönberg, A.; Mustafa, A. *J. Chem. Soc.* **1943**, *33*, 79.
55. Behaghel, O.; Freiensehner, H. *Ber.* **1934**, *67*, 1368.
56. Given, P. H.; Hammick, D. L. *J. Chem. Soc.* **1947**, 1237.
57. Monacelli, W. J.; Hennion, G. F. *J. Am. Chem. Soc.* **1941**, *63*, 1722.
58. Himbert, G.; Fink, D. *J. Prakt. Chem./Chem. Ztg.* **1997**, *233*, 339.
59. Dann, O.; Kokorudz, M. *Chem. Ber.* **1958**, *91*, 1712.